

# IR UPGRADE WITH QUADRUPOLES FIRST AND DIPOLES FIRST\*

T. Sen, J. Johnstone, V. Ranjbar<sup>1</sup>, FNAL, Batavia, IL 60510, U.S.A  
R. Tomas-Garcia, CERN, Geneva, Switzerland.

## Abstract

We review recent work on the LHC IR upgrades by the US-LARP collaboration. There are several optics designs under consideration – each design differs in the potential luminosity reach, accelerator physics, operational and technical challenges. Here we consider the likely benefits of moving the IR magnets closer to the IP for both quadrupole-first and dipole-first designs. The impact of beam-beam interactions in the two designs is analysed for the first time. We conclude with a summary of accelerator physics parameters for the two designs.

## INTRODUCTION

The baseline quadrupole-first design and two flavors of the dipole-first design studied by the US-LARP collaboration were discussed at the Luminosity 2005 workshop [1]. The two dipole-first designs under study feature: (1) triplet focusing with anti-symmetric optics and (2) doublet focusing with symmetric optics in the inner IR magnets. Doublet optics leads to a larger luminosity at the cost of producing elliptical beams at the IP and enhanced chromaticities. Table 1 shows the required aperture and peak fields in the inner IR magnets at collision optics for the three designs.

	Pole tip field [T]	Aperture [mm]
Quads 1st	10	101
Dipoles 1st: triplets	11	107
Dipoles 1st: doublets	10	104

Table 1: Maximum pole tip field and apertures required in the IR magnets at collision optics.

The requirements on the aperture are about the same in all designs even though the beta functions are about three times larger in the dipole-first designs. Both beams are accommodated within a single aperture in the quadrupole-first designs while the beams are separated into different apertures in the dipole-first designs. The optics and layout will be discussed in the following sections. The optics of the insertions has been matched into the complete LHC ring by R. Tomas-Garcia. The MADX files of the complete lattices are available on the LHC upgrade repository [2].

A complete IR design requires study of related accelerator physics issues including but not necessarily limited to: optically matched designs at all stages of the operational cycle, correction of linear and non-linear chromaticity of the insertions, correction of the non-linear fields of the IR magnets, the impact of beam-beam interactions,

energy deposition in the magnets from the collisions at the IP, correction of dispersion within the IR, susceptibility to alignment errors, power supply noise, ground motion etc.

A critical parameter that affects all these issues is the distance of the first magnet from the IP. At the Luminosity 2005 workshop there was some discussion with experimenters from Atlas and CMS about the feasibility of placing magnets inside the detectors. In the following sections we explore how moving magnets closer to the IP might improve the IR performance. We also take a first look at the impact of beam-beam interactions in the different designs.

## QUADS FIRST

The optics functions through an insertion with  $\beta^*=0.25\text{m}$  are shown in Figure 1. The layout is unchanged with  $L^*$  (distance to the first quadrupole) = 23m as in the baseline design. The vertical dispersion at IP5 is created by the vertical crossing angle at IP1. The maximum  $\beta$  is about 9km, about twice the baseline value.

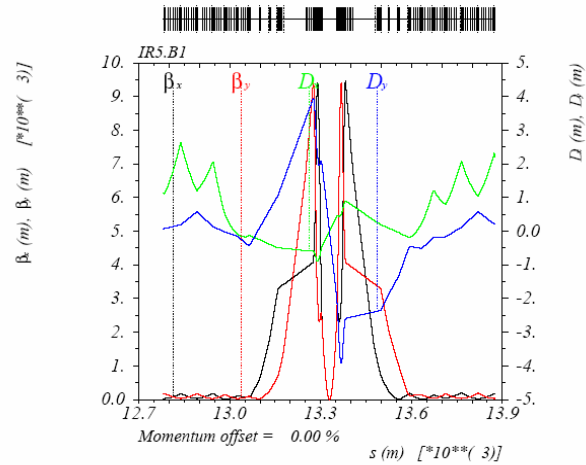


Figure 1: Plot of the twiss functions through IR5 with the quadrupole-first optics.

## Variation with $L^*$

Moving the magnets closer to the IP reduces the  $\beta^{\max}$  for the same value of  $\beta^*$ . Conversely, keeping  $\beta^{\max}$  constant allows us to reduce  $\beta^*$  for a potential gain in luminosity at lower  $L^*$ . For this exercise we adopted a shorter version of the insertion extending from Q4 on the left to Q4 on the right. The optics at these quadrupoles was matched to nearly the same values as in the complete insertion at  $\beta^* = 0.25\text{m}$ . The gradients are kept the same

<sup>1</sup>Now at Tech-X, Boulder, CO

but the quadrupole lengths are changed to reduce  $\beta^*$  to the lowest possible value keeping  $\beta^{\max}$  constant at each value of  $L^*$ .

The luminosity depends directly on  $\beta^*$  as  $1/\beta^*$  and indirectly through the crossing angle. As  $\beta^*$  is decreased, for the beam separation to stay constant, the crossing angle must increase as  $1/\sqrt{\beta^*}$  which reduces the luminosity. If  $L^*$  decreases by more than half the bunch spacing, the number of parasitic interactions also falls. In such cases we can take advantage of an empirical scaling by Papaphilippou and Zimmerman [3] which suggests that the crossing angle scales as  $\sqrt{N_{LR}}$  where  $N_{LR}$  is the number of parasitic interactions.

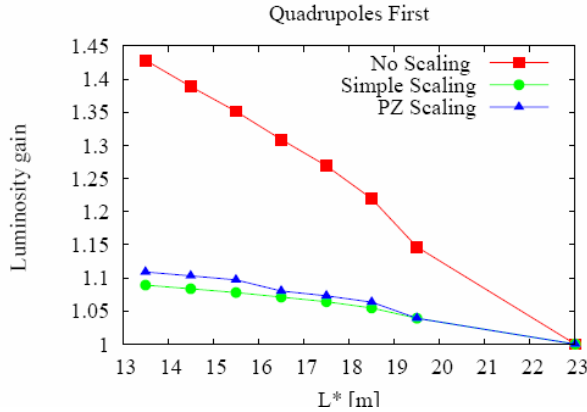


Figure 2: Luminosity vs.  $L^*$ ; quads-first

The luminosity at each  $L^*$  can be calculated after  $\beta^*$  is found from optical matching. The dependence of the luminosity on  $L^*$  is shown in Figure 2 for three different cases. The case “No scaling” does not take into account the dependence on the crossing angle. This might be appropriate if some means of beam-beam compensation is found which allows the crossing angle to stay constant. The difference between simple scaling (only the crossing angle but not the dependence on  $N_{LR}$ ) and PZ scaling [3] is not significant. The luminosity gain by reducing  $L^*$  to 13m is about 11% if the crossing angle dependence is included while the gain is nearly 45% if the crossing angle can be allowed to stay constant. This result clearly shows that reducing the  $L^*$  in itself will not significantly increase the luminosity unless the parasitic beam-beam interactions are compensated to allow for the same or smaller crossing angle.

As the quadrupoles are moved closer to the IP, their focusing strength also increases. Consequently, the chromaticity of the inner triplet also increases with shorter  $L^*$ . Figure 3 shows the change in chromaticity – about 4 units per IR per plane as  $L^*$  is reduced from 23m to 13m.

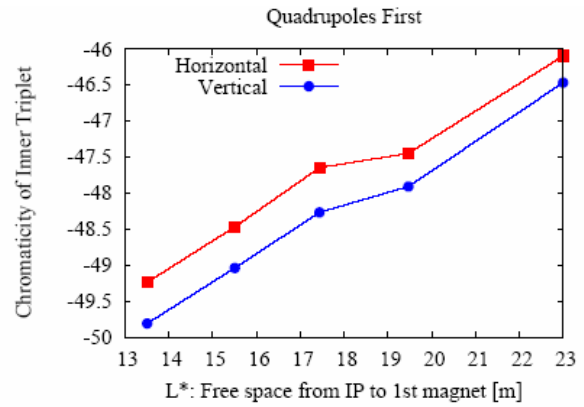


Figure 3: Chromaticity vs.  $L^*$ ; quads-first

### Beam-beam effects

We now analyse the beam-beam interactions with  $L^* = 23\text{m}$  and  $\beta^* = 0.50\text{m}$  (baseline) and  $\beta^* = 0.25\text{m}$  (upgrade). At  $\beta^* = 0.25\text{m}$ , the crossing angle is increased to  $400\mu\text{rad}$  from the baseline value of  $285\mu\text{rad}$ . Figure 4 shows the tune footprint (calculated analytically) up to  $6\sigma$  when the head-on interactions and 30 long-range interactions each at IP1 and IP5 are included. The footprints are nearly the same since the beam separations (in units of  $\sigma$ ) are almost the same.

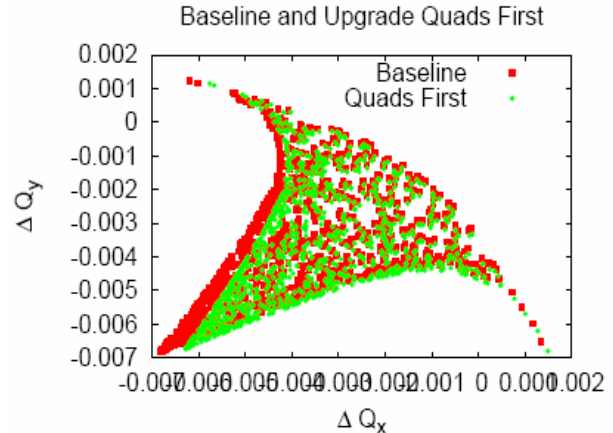


Figure 4: Beam-beam tune footprints to  $6\sigma$ .

Resonance driving terms can also be used to characterize the strength of the non-linearity. With the LHC working point at  $(0.31, 0.32)$ , the nearby low-order resonances are the 3<sup>rd</sup> and 10<sup>th</sup>. Figures 5 and 6 show the magnitudes of the strongest 3<sup>rd</sup> and 10<sup>th</sup> order resonance driving terms at each of the parasitics in IR5, evaluated at amplitude of  $6\sigma$ . The analytical expressions may be found in Reference [4]. Perhaps due to differences in matching, the beam separations (again in units of  $\sigma$ ) in the drift space are slightly different in the two lattices. Since higher order resonances are more sensitive to beam separations, the differences are amplified for the 10<sup>th</sup> order resonances. When all the parasitics are included, the beam-beam resonance driving terms in the baseline and the upgrade lattice are not significantly different.

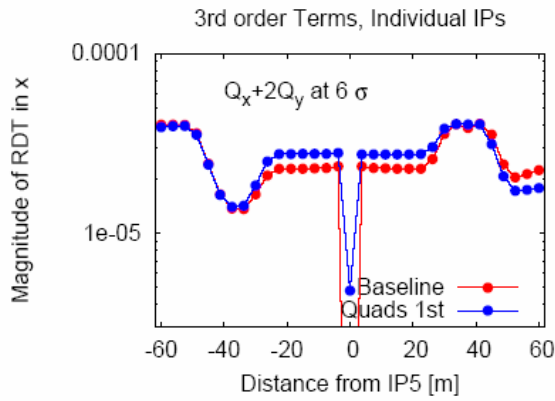


Figure 5: Beam-beam  $Q_x+2Q_y$  resonance driving term magnitude in the baseline and upgrade at each parasitic interaction in IR5.

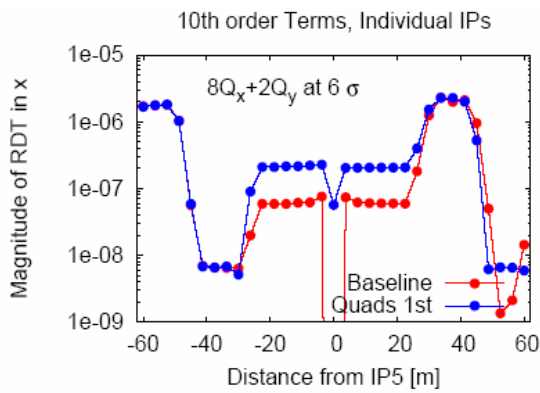


Figure 6: Beam-beam  $8Q_x+2Q_y$  resonance driving term magnitude in the baseline and upgrade at each parasitic interaction in IR5.

Simulations can also probe the impact of the beam-beam interactions. We have used the code BBSIM developed at FNAL [5] to calculate the diffusion coefficients at different amplitudes. Figure 7 shows the horizontal diffusion coefficient  $D_x$  as a function of the horizontal amplitude  $A_x$  for the two lattices and similarly Figure 8 shows the dependence of  $D_y$  on  $A_y$ .

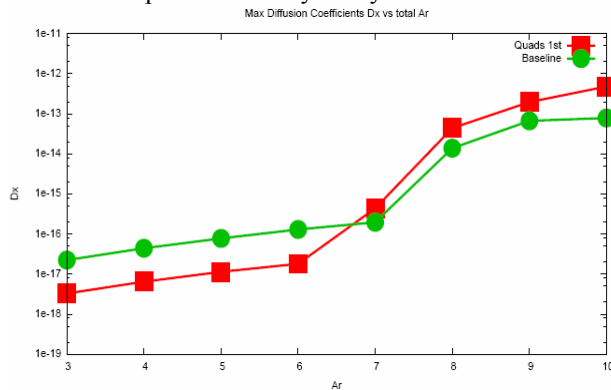


Figure 7: Diffusion coefficient  $D_x$  in the horizontal plane vs. amplitude for the baseline and upgrade optics.

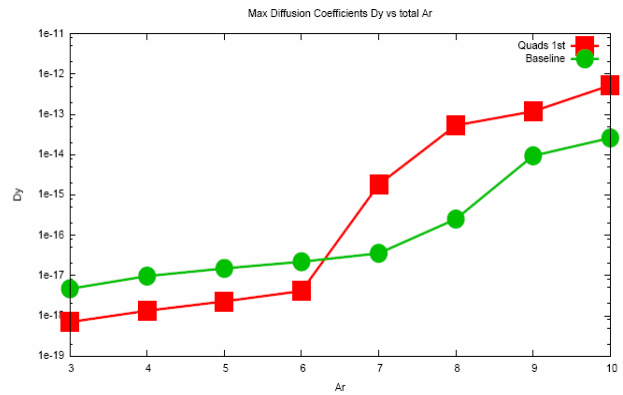


Figure 8: Diffusion coefficient  $D_y$  in the vertical plane vs. amplitude for the baseline and upgrade optics.

The dependences of  $D_x$  on  $A_y$  and that of  $D_y$  on  $A_x$  are not shown here – the differences are less significant. We observe that the diffusion jumps at  $8\sigma$  in the baseline lattice but the jump occurs at  $7\sigma$  in the upgrade lattice. This suggests that the beam-beam interactions will further limit the dynamic aperture in the upgrade. This makes the need for beam-beam compensation stronger.

## DIPOLES FIRST

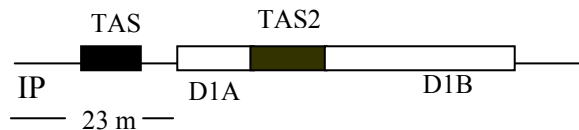


Figure 9: Layout of the TAS absorbers with dipoles-first. Sketch is not to scale.

We will mainly use the dipole-first triplet focusing layout and optics to compare with the quadrupoles-first layout. The special design required for the D1 dipole magnet to cope with the energy deposition was discussed in Reference [1]. A total field of 20 T-m is required to deflect the charged particle debris into a second absorber TAS2. Figure 9 shows the layout. The 10m long D1 dipole is split into two with D1A of 1.5m length (hence strength 20 T-m) and D1B of 8.5m length. We also place a 5m long neutral absorber TAN after the second separation dipole TAN. As a consequence, the first quadrupole Q1 is moved back to 55.5m from the IP compared to 23m in the quadrupole-first layout. This consequently increases the beta functions at the quadrupoles. The twiss functions through the insertion are shown in Figure 10. The maximum beta function increases to about 27km.

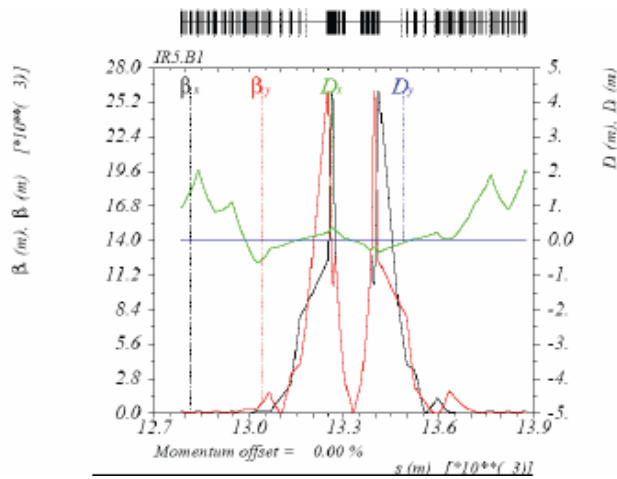


Figure 10: Twiss functions through IR5 at collision with dipoles first, triplet focusing.

### Variation with $L^*$

The potential luminosity reach of the dipoles first optics by reducing  $L^*$  was studied similarly as for the quadrupole-first optics. The part of the insertion between the Q4s was used;  $\beta^{\max}$  was kept constant while matching to the lowest  $\beta^*$  at each value of  $L^*$ . Since the quadrupoles are much further back in this optics,  $\beta^*$  values are higher for the same shift towards the IP.

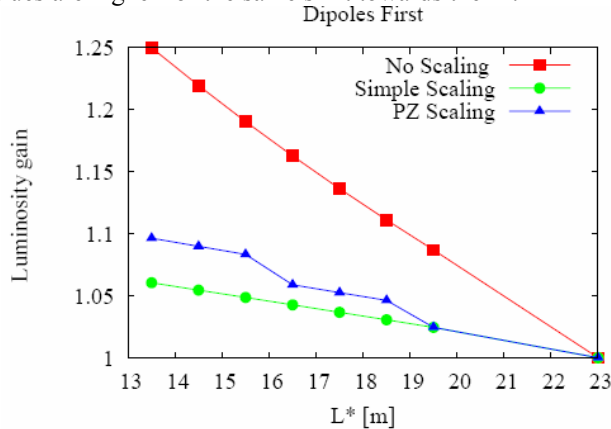


Figure 11: Change in luminosity as D1 is moved from 23m to 13m from the IP; dipole-first optics, triplet focusing.

Figure 11 shows the gain in luminosity as the magnets are moved closer to the IP. In this figure the horizontal axis is the distance of D1 from the IP. For the case of “no scaling”, i.e. no change in crossing angle with distance, the gain in luminosity is about 25% at 13m. The gain in luminosity in the other two cases when the crossing angle is increased at smaller  $L^*$  is limited to 10% at 13m. There is at least one caveat in comparing these results with the quadrupoles first layout. Due to the smaller number of parasitic interactions with dipoles first, a smaller crossing angle might suffice which would increase the luminosity.

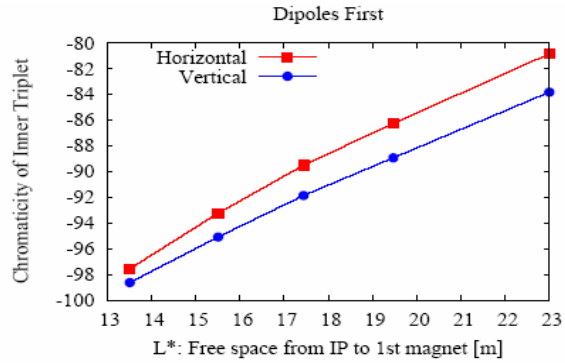


Figure 12: Change in chromaticity with  $L^*$ ; dipoles first, triplet focusing.

The chromaticity is higher in the dipoles first layout because of the higher  $\beta$  functions. Figure 12 shows that as the D1 dipole is moved from 23m to 13m the magnitude of the chromaticity increases by about 20 units per IR per plane. Reducing  $L^*$  in this fashion (keeping  $\beta^{\max}$  constant) would significantly increase the sextupole strengths. Since the apertures stay constant, this strategy can be physically realized without changing the quadrupoles. Other strategies can be envisaged, e.g. keeping the chromaticity constant while reducing  $L^*$ . The aperture requirements would change with  $L^*$ .

### Beam-beam calculations

The chief advantage of the dipoles first layout is the smaller number of parasitic beam-beam interactions. The beams are in separate beam pipes when they enter the quadrupoles. Figure 13 shows the beam separation in the baseline layout and in the dipoles first layout. In the latter, the beam separation stays constant at  $9.4\sigma$  (crossing angle =  $400\mu\text{rad}$  at  $\beta^* = 0.25\text{m}$ ).

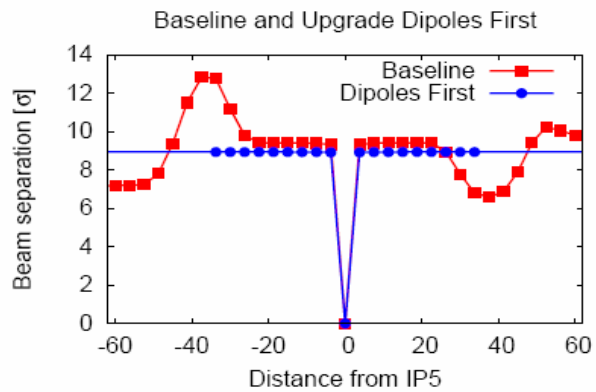


Figure 13: Beam separation at the parasitic interactions in the baseline and the upgrade.

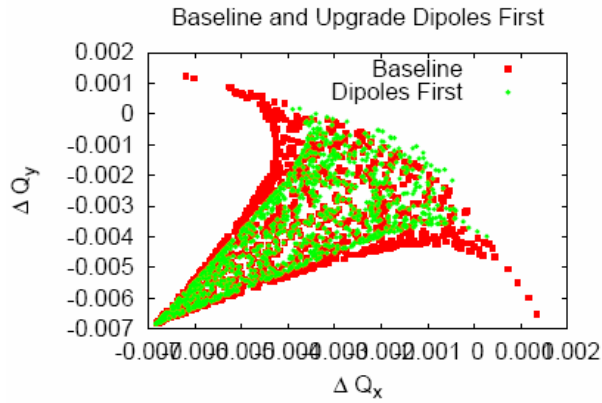


Figure 14: Beam-beam tune footprint in the baseline and dipole-first layout, triplet focusing.

As expected, the beam-beam tune footprint, seen in Figure 14, is smaller especially at amplitudes greater than  $3\sigma$ . The largest 3<sup>rd</sup> and 10<sup>th</sup> order resonance driving terms are shown in Figure 15 and 16. Summed over all the interactions, the resonances are weaker in the dipoles first layout because of the fewer parasitics but mainly because there are no parasitics at the smallest separations of about  $7\sigma$  as there are in the baseline.

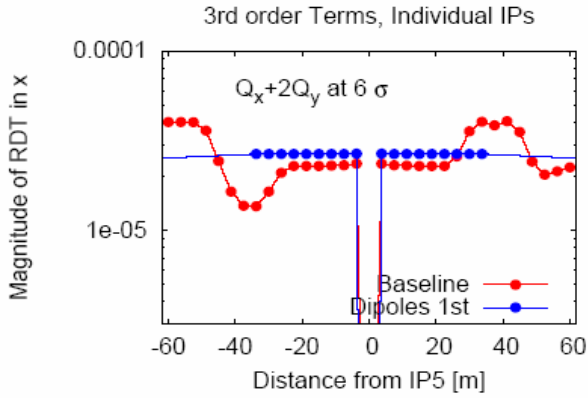


Figure 15: Largest 3<sup>rd</sup> order resonance driving terms in the baseline and the dipole-first layouts

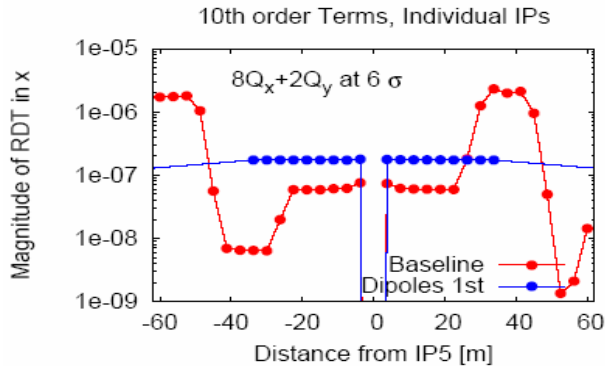


Figure 16: Largest 10<sup>th</sup> order resonance driving terms in the baseline and the dipole-first layouts.

Simulations with BBSIM of the diffusion due to the beam-beam interactions also show the improvement in the dipoles first layout compared with the baseline. Figure 17 and 18 show the horizontal and vertical diffusion coefficients respectively for all three layouts. At amplitude up to  $7\sigma$ , the diffusion coefficients in the dipoles first case are smaller by about two orders of magnitude. There is a jump in the diffusion at  $8\sigma$  in both cases and at larger amplitudes the difference in diffusion is less significant.

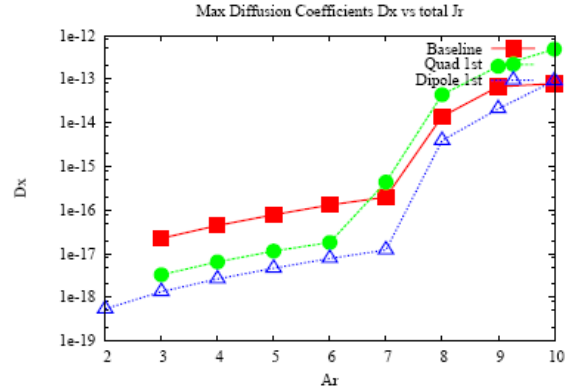


Figure 17: Horizontal diffusion coefficient  $D_x$  vs. the radial amplitude  $A_r$  for all three layouts.

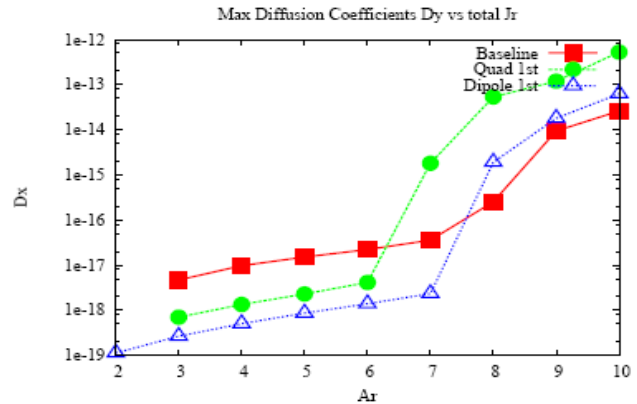


Figure 18: Vertical diffusion coefficient  $D_y$  vs.  $A_r$  for all three layouts.

### Doublet focusing vs. Triplet focusing

Doublets create optics with  $\beta_x^* \neq \beta_y^*$ . This can be used to advantage by having  $\beta_x^* > \beta_y^*$  when the crossing plane is horizontal and benefit from the larger luminosity compared to the situation with  $\beta_x^* = \beta_y^*$ . However the parasitic interactions are stronger in this optics, e.g. the tune footprint is larger [1]. A separate strong-strong simulation by J. Qiang (LBL) shows that the emittance growth from head-on collisions is higher with elliptical beams (doublets) than with round beams (triplets). IRs with doublet optics also have higher chromaticities than with triplets. The higher luminosity with the doublets exacts a steep price in terms of other beam phenomena.

## SUMMARY

We have compared several aspects of the quadrupoles first and dipoles first layouts. The apertures and pole tip field requirements are about the same in all layouts: apertures  $\sim 110$  mm, pole tip field  $\sim 11$  T. Chromaticities are higher with dipoles first. The beam-beam interactions are weaker with dipoles first as expected, e.g. diffusion is about two orders of magnitude smaller at amplitudes up to  $7\sigma$ . Recent energy deposition simulations with the two layouts show that the energy deposition in the quadrupoles is smaller with dipoles first and can be mitigated even at luminosities of  $10^{35}\text{cm}^2\text{sec}^{-1}$  [6]. This presumes however that the challenging open mid-plane magnet design proposed for D1 is feasible. Table 2 summarizes the key parameters of the comparison between the layouts.

	Quads 1st	Dipoles 1st
Lowest $\beta^*$ at $L^* = 19\text{m}$	0.22	0.23
Lumi gain at $L^*=19\text{m}$ vs. $L^*=23\text{m}$	1.04 – 1.15	1.02 – 1.09
$L^* = 23\text{m}$		
$\beta^{\text{Max}}$ [m] at $\beta^* = 0.25\text{m}$	9484	26092
Max aperture [mm]	101	107
Max pole tip field [T]	10.1	10.7
Q' of inner quads	-48	-99
Max 3rd order bb resonance	$0.9 \times 10^{-3}$	$0.5 \times 10^{-3}$
Max 10th order bb resonance	$0.16 \times 10^{-3}$	$0.3 \times 10^{-5}$
Beam-beam diffusion	Jump at $7\sigma$	Jump at $8\sigma$
Max Energy Deposition in quads [mW/g]	1.0	0.6

Table 2: Comparison of the main features in the quadrupoles-first and dipoles-first layouts.

We also compared the luminosity gain by reducing  $L^*$  in both layouts. While  $\beta^*$  can be reduced to 0.17m with quadrupoles first and 0.20m with dipoles first at  $L^* = 13\text{m}$ , the gain in luminosity is limited due to the need for increasing the crossing angle as  $1/\sqrt{\beta^*}$ . Active beam-beam compensation of the parasitic interactions would improve the performance and the luminosity gain.

## REFERENCES

- [1] T. Sen et al. "US-LARP Progress on LHC IR upgrades", Proceedings of the Lumi 05 workshop, Arcidosso, 2005
- [2] LHC IR Upgrade Lattice Repository <http://>
- [3] Y. Papaphillipou and F. Zimmerman, Phys. Rev. ST AB Vol (200X) page.
- [4] T. Sen et al., PRSTAB, Vol (2004) page
- [5] BBSIM web site
- [6] N. Mokhov et al, this workshop